Dynamic Drop Testing of eVTOL Energy Storage Systems Part 1: Drop Test Data Summary

Justin Littell
Research Aerospace Engineer
NASA Langley Research Center
Hampton VA, 23681

Nathaniel Gardner
Research Aerospace Engineer
NASA Langley Research Center
Hampton VA, 23681

Shay Ellafrits
Research Aerospace Engineer
NASA Glenn Research Center
Cleveland OH, 44135

ABSTRACT

Researchers at the National Aeronautics and Space Administration (NASA) have conducted a series of module-level tests on electric Vertical Take-off and Landing (eVTOL) Energy Storage Systems (ESS) for the generation of dynamic impact data to support standards developments. The tests were conducted on zero-state-of-charge Electric Power Systems (EPS) Electric Propulsion Ion Core (EPIC) modules at the National Institute for Aviation Research (NIAR), utilizing the NIAR outdoor drop test setup and personnel. Four total tests were conducted. For each test, the module was dropped at a specific orientation from a height of 50 feet while connected to a guided trolley in order to assess the effects of a 50-foot drop test on the ESS. The test velocities ranged between 46.9 and 52.8 ft/s with impact angles ranging between a flat, zero-degree impact and 18 degrees. Data were recorded in the form of temperatures, cell-level voltage, module level acceleration and digital image correlation from the tests. Accelerations were in the range of 1,500 g for a few millisecond duration, which were indicative of a shock type loading condition. No modules entered thermal runaway, and post-test inspections revealed a variety of internal deformations and damage present in the various modules tested, with specific damage occurring for specific orientations. The modules were ranked according to a custom developed scoring rubric developed by utilizing the test and post-test inspection results. The results were compiled, reported, and will be used to guide future ESS testing. Part 1 discusses the loading environments in the modules, while Part 2 will discuss the deformation and damage in the modules.

Introduction

Electric Vertical Take-off and Landing (eVTOL) vehicles are poised to change the paradigm for transportation in the urban environments by providing services including supporting disaster relief, medical transport, package delivery as well as being able to transport people much like how taxi services operate currently. New vehicles, currently in development, are tailored to these types of environments and missions by utilizing novel materials, design features and propulsion. One main feature of these vehicles is the use of hybrid or fully-electric power systems along with a variety of lift generating devices as their primary means of propulsion. The electric power systems will consist of large amounts of battery modules typically containing battery cells connected to onboard battery management systems, cabling, sensors and other associated hardware. These battery components are often grouped under the general term *Energy Storage Systems (ESS)*.

In order to be able to operate these types of aircraft in the airspace of the United States, all aircraft systems must be certified for airworthiness. Due to the new and unique nature of the hybrid and fully electric power systems, there are gaps in the current certification requirements for a variety of the eVTOL components. Specifically for the ESS, no current regulation directly covers the certification for crashworthiness of the ESS when used *as the primary means of propulsion* on aircraft in the United States. The most applicable regulation is found in the regulations for rotorcraft (both Normal and Transport categories) as a part of the fuel system requirements. Specifically, it is found in Code of Federal Regulations Title 14 part 27 section 952 (14 CFR § 27.952) [1] "Fuel System Crash Resistance," which stipulates that the most critical fuel tank must survive from being drop tested from a height of 50 feet. Successfully passing this test (and many others not related to crashworthiness) is critical for being able to certify these fuel systems for flight. Attempts to use this

Presented at the Vertical Flight Society's 81st Annual Forum & Technology Display, May 20-22, 2025, Virginia Beach, Virginia.

requirement for eVTOL vehicles are currently ongoing because of this gap in ESS certifications.

There are two examples [2][3] in the Federal Register that discuss eVTOL certification under 14 CFR §21.17 paragraph (b) [4], which is intended for "*special classes of aircraft … for which airworthiness standards have not been issued*". This method intends to pull requirements from various current parts of the regulations including 14 CFR § 23, 25, 27 29, 31, 33, and 35, along with adding a handful of requirements which would be vehicle specific. There is discussion text for both examples which stipulates that a new requirement for ESS will be introduced which "*would include a requirement to address energy system crashworthiness to capture the intent of § 27.952 and would delete requirements specific to liquid fuel systems*." The proposed additional text is identical for both and states *"Each energy system must be designed to retain energy under all likely operating conditions and to minimize hazards to occupants following an emergency landing or otherwise survivable impact (crash landing)."* In either case, a proposed Means of Compliance is not stipulated nor specific guidance on performance needed to pass the criteria is given. It should be noted that the European Union Aviation Safety Agency (EASA) has accepted the 50-foot drop test (Section MOC VTOL.2325(a)(4)) as a suitable Means of Compliance in their Special Condition VTOL document [5].

As a part of the Revolutionary Vertical Lift Technology (RVLT) project, NASA has undertaken a research program that will evaluate an ESS module performance under a variety of configurations through the conduct of vertical drop testing. It is important to note that the research objectives are not to certify the ESS modules against any proposed or actual certification requirement, but rather use the tests to help determine fundamental factors, failure modes and mechanisms associated with ESS modules that result from impact testing under the various configurations. The insight gained is intended to guide future efforts into protecting the structures against a variety of types of impacts, to develop rationale for proposed test conditions and provide the community with information resulting from the tests. The research is being conducted in three phases. The first phase, which will be discussed in this report, will evaluate eVTOL ESS under a variety of orientations in 50-foot drop tests without external attenuation or structure. Phases 2 and 3 will build from the results in Phase 1 and will be presented in future publications. For Phase 1, the reporting will be divided into two parts. Part 1, which is described herein, will discuss the general test setup, along with presenting data which will evaluate the loading environment for each of the tests conducted. Post-test forensics which include inspections and teardowns, along with photogrammetric results documenting the impact and post-test deformations, will be the primary focus and presented in Part 2 [6].

TEST ARTICLES

Testing was conducted on Electric Power Systems (EPS) Electric Propulsion Ion Core (EPIC) Energy Modules. Each module weighed approximately 24.5 lb. and can generate 2.3 kWh of power. All modules were designed to TSO-179b [7] and UN38.3 [8] requirements. The modules were tested in a zero-state-of-charge configuration, which was chosen to minimize - but not eliminate - the threat of thermal runaway (TR) during the tests. The threat of thermal runaway was minimized in order to safely conduct post-test teardowns and forensics to determine and document what types and where damage was located in the modules, should damage be present. The EPIC Energy Module is shown in Figure 1. There is a red protective covering over the vent port of the module, which was removed during testing.

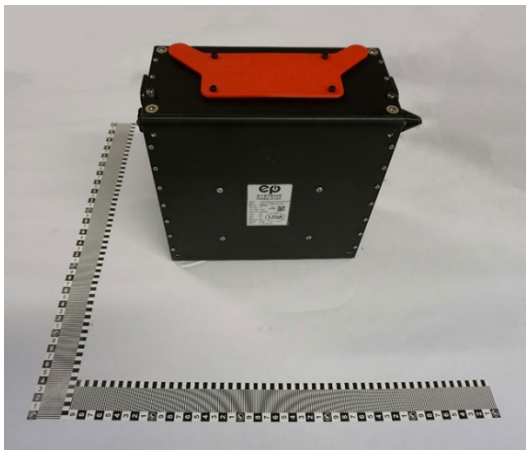

Figure 1. EPS EPIC ESS Module

The test series consisted of conducting four drop tests. Four individual modules were tested with each module being tested once, and in a specific orientation. The four orientations tested (with reference to the vent port) were: Rightside Up, Upside Down, Sideways, and Flatwise. The two remaining directions were symmetric to those being tested and therefore not evaluated. Diagnostic measurements were conducted to monitor the health of the modules both before and after the drop tests. These measurements collected

information about cell voltage and temperature along with continuity between the various cells within the modules itself.

TEST SETUP

The testing conducted for this study follows the guidance identified in 14 CFR § 27.952 [1], and uses a suggested test procedure identified in ref. 9. In each test, the module impacted a rigid surface with no surrounding structure or attenuation present. Guidance uses the text "within structure" to best replicate the installed condition, however, there were two primary reasons for conducting the tests on the modules by themselves. The first was to answer the questions proposed in the *Introduction* section of this report, and the second was to replicate, to the best extent possible, a potential condition where the ESS may be installed in a configuration which may not have any significant attenuation.

The tests were conducted at that National Institute for Aviation Research (NIAR) at NIAR's outdoor drop test facility by NIAR test personnel. The test apparatus used to lift and drop the test articles was a trolly and guide wire system developed by NIAR which has been used for previous ESS tests [10]. Each test article was suspended under the trolly via cables, and the trolley was lifted into the air such that the test article was at a height of 50 ft from a rigid impact surface. Upon release, both the trolly and the test article fell along guide wires toward the impact surface. The test article was connected to the trolly such that it made contact with the impact surface prior to the arrestment system on the trolly activating. Thus, a nearly free fall onto rigid surface test condition was achieved.

Acceleration, temperature, and deformation were the primary data that were collected for each test. Each module was instrumented with three accelerometers and four thermocouples. Two accelerometers with 20,000-g full-scale range were mounted externally on the Enclosure Assembly at two opposite corners on or near the upward facing surface, while a third 2000-g accelerometer was mounted in the middle of the upward facing surface. The two 20,000-g accelerometers will be referred to as SN 1631 and SN 1632 while the 2000-g accelerometer will be referred to as *Accel 2000*. These locations were chosen specifically to measure the response from both the more rigid (corners) and unsupported/compliant (middle) locations of the modules, while also being able to capture any off-nominal impact events that should occur and/or document timing of particular events, should that be needed. Two thermocouples were mounted on the non-painted side surface and two were mounted on the upward facing surface, though their specific locations were not tightly controlled. A simple view of the instrumentation applied to a test article is shown in Figure 2.

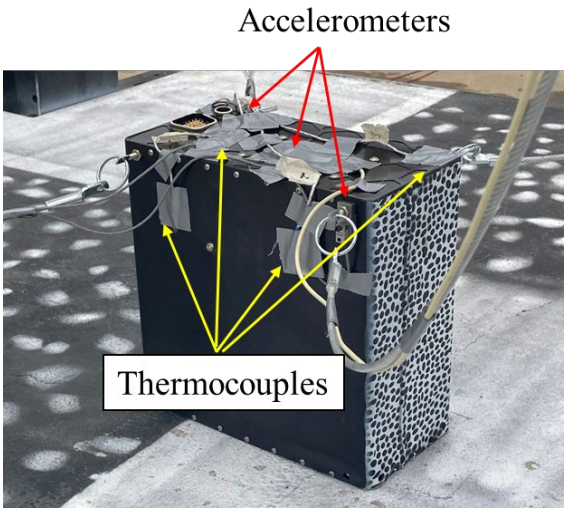

Figure 2 - Module Instrumentation

All accelerometer and thermocouple data were collected via an offboard data acquisition system recording data at 100 kHz. The data will be presented identified by the directional (North, South, East, West) orientations of the test articles at the test site. Since each test was a unique configuration, it was not possible to control the module directional orientation such that it was the same for all test conducted, and thus locations may not be similar between tests So while the data was collected to identify the locations of the measurements collected on the modules during each test, the results presented will use the data as referenced to either these directions or using the test articles themselves.

For each module, two surfaces were painted with a stochastic speckle pattern for use in high-speed photogrammetry, specifically deformation tracking via digital image correlation techniques. The main objective of the photogrammetry was to determine deformation of the module enclosure during the impact event, along with confirming impact velocity and angle using yellow and black "bowtie" targets. High speed camera resolution was typically 1 megapixel and the collection rate ranged between 5 and 10 kHz. Additional infrared and real-time cameras were utilized to observe each test. The photogrammetry data will be discussed in detail in Part

2. An example of two painted surfaces from a test article is shown in Figure 3.

Figure 3 - Module paint for photogrammetry

Immediately after each impact, the test article was left in its post-test condition, undisturbed, for 1 hour. Temperatures from the mounted thermocouples were monitored and recorded over the course of the hour and if an uncontrolled temperature rise was observed (a potential indication of TR), the test article would be moved from the impact site and submerged into a large dunk tank. If the test article temperatures appeared stable during and after the one-hour observation period, the test article was then approached, and post-test inspections began. The post-test inspections included observations noting the general condition of the test article, the presence of electrolyte (smell) and the signs of spark, smoke or flame (visual). In addition, as previously noted, information regarding internal temperature and cell voltages (if available) were recorded. After the post-test inspections, the test articles were moved from the test site into outside enclosed storage. After 24 hours in outside storage, the test articles were again examined for changes in temperature or condition. If no change was observed, the test article was ready for post-test forensics. The drop test setup, with the test article at the beginning of the lift and at the end of the lift is shown in Figure 4 and Figure 5, respectively.

Figure 4 – Test article at beginning of lift

Figure 5 - Test article at end of lift

RESULTS

Flatwise Orientation

For the Flatwise orientation test, the test article was placed such that the top vent facing perpendicular to the impact surface, and oriented such that the vent port was facing South, and the positive electrode was facing West. Accelerometer SN 1631 was placed in the northeast corner of the enclosure and SN 1632 was placed in the southwest corner. Accel 2000 was positioned in the middle of the upward facing side, near the identification placard of the module. The end with the negative electrode and the bottom were painted with the stochastic pattern and the test article was attached to the trolley via cables attaching to the upward facing side.

The test was conducted on November 14, 2023, at 12:32 PM local time. The outside temperature was 68.3° F with a relative humidity of 35.6%. Winds were 6 miles per hour (MPH) gusting to 10 MPH. The test article impacted at the north-west corner, with a north side low angle of 17.9 degrees, west side low angle of 1.4 degrees and an impact velocity of 46.9 feet per second (ft/s). A test sequence from the flatwise test is shown in Figure 6.

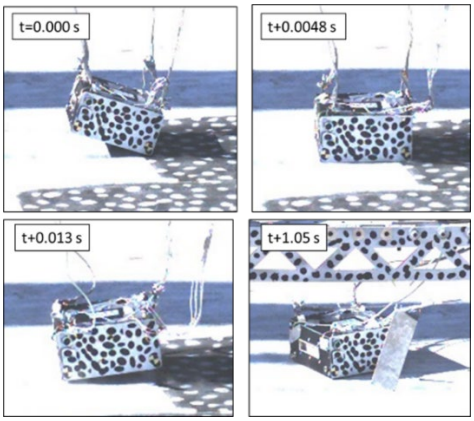

Figure 6. Test sequence - Flatwise orientation

The view in Figure 6 is looking from the east, at the side containing the negative electrode. The image sequence shows a counter-clockwise rotation through the impact, starting with the north-side initial impact in the upper left image. The base of the test article was on the north side, so the base of the test article impacted first, which then rotated counterclockwise with the top of the test article impacting 4.8 milliseconds (ms) later. After the top impacted, the test article rebounded while still undergoing counterclockwise rotation. The time of the start of the rebound is shown in the lower left image. The rebound, which was restrained by the attachment cables, lasted approximately 1 second, after which the test article came to rest, slightly rotated toward the west, and laying on the original impact side. The test article in its post-test position is shown in Figure 7.

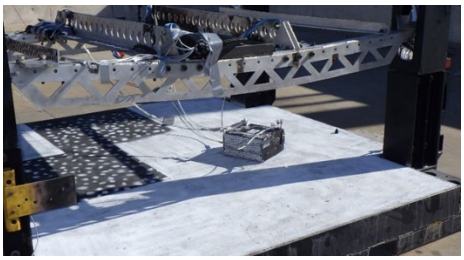

Figure 7 - Post-test position, Flatwise orientation

The acceleration data from this test are shown in Figure 8.

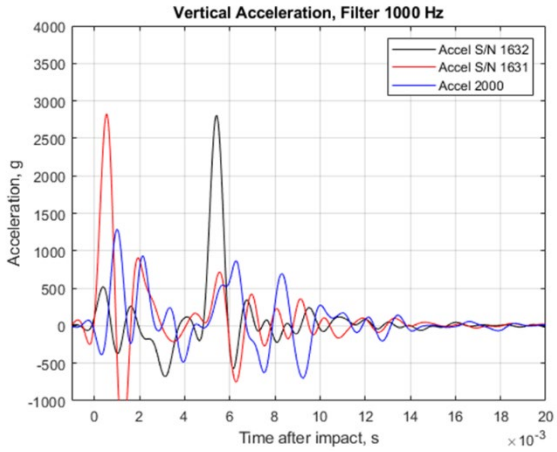

Figure 8 - Acceleration from Flatwise orientation

The data for this test and all others are plotted utilizing a forward and backward 4-pole 1000 Hz low-pass Butterworth filter, and not the typical SAE J211 [11] filtering methods. The higher filter was required due to the extreme short duration and other pulse characteristics that were measured during the test. Various cut-off frequencies were examined (not included in this report) and it was determined 1000 Hz was the lowest suitable value because it only resulted in a 2.7% signal difference in the initial spike and a 1.4% difference in the entire pulse. Any lower frequency significantly underpredicted the initial spike and had an increasingly higher percentage of signal loss. Thus, all data presented in this report will use the 1000 Hz frequency for results reporting, unless otherwise noted.

Finally, with all plots that will be shown in this report, a time of zero indicates the time in which the test article first contacted the impact surface and is typically determined by the examination of the high-speed video. Thus, all times referred to in this report will be referenced to this initial impact time of zero.

There are two distinct peaks on the acceleration plots, which align with the two distinct impact events of the test. The red spike, which corresponds to accelerometer SN 1631 on the north side of the test article, appears at impact and measures a magnitude of 2,820 g while the black spike, which corresponds to accelerometer SN 1632 placed on the south side of the test article, measures a peak value of 2,802 g and occurs 4.8 ms after the impact. There are two distinct spikes due to the large non-zero impact angle, leading

to the two sides impacting at slightly different times. These spikes have extremely high magnitude due to two factors. The first was the orientation of the impact, causing each side to impact separately at slightly different times, and the second was because they were mounted at the corners of the modules, which were the stiffest locations in the enclosure. The accelerometer mounted on the center of the module, Accel 2000, measured a peak acceleration of approximately 1,285 g 1 ms after impact, which was approximately half of the measured values at the corners, and approximately in the middle, timing-wise, of the side impacts. The impact from each side was also measured in Accel 2000, which does show small spikes at the timing of the side impact. However, the magnitudes were all in the same range, indicating the middle location was likely a better location to measure the overall response in the module.

The post-test diagnostics were able to confirm readings for post-test voltages and temperatures indicating connectivity was present in the module post-test. This result suggested the internal damage (if any) in the module was minor enough to allow for the internal connections to be intact, or in locations not affecting the continuity connections. The thermocouple data did not show any significant temperature rise in the test articles posttest, so it was determined no TR was occurring. However, per the test procedure, the module was left in outside storage for monitoring for a period of 24 hours. After the 24-hour monitoring period, the test article was ready for post-test forensics.

Rightside Up Orientation

The Rightside Up orientation positioned the test article with the vent facing upward and opposite of the impact surface and oriented the test article such that the positive electrode was facing West. Accelerometer SN 1631 was placed in the northeast corner of the test article, while SN 1632 was placed in the southwest corner. Accel 2000 was placed on the top surface near the vent. The sides with the positive electrode and identification placard were painted with the stochastic speckle pattern. The test was conducted on November 14, 2023, at 3:26 PM local time. The outside temperature was 68.2° F with a relative humidity of 34.8 %. Winds were 5.7 MPH gusting to 12.3 MPH. The test article impacted at the south-east corner, with a south-side low angle of 2.2 degrees, east-side low angle of 2.6 degrees and an impact velocity of 52.8 feet per second (ft/s). A test sequence from the Rightside Up test is shown in Figure 9.

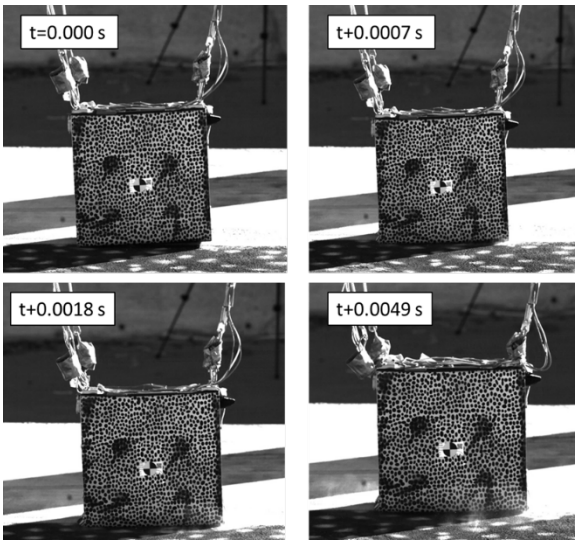

Figure 9. Test sequence - Rightside Up orientation

The test article impacted at a slight left side low (east) angle. Due to the low but non-zero impact angle, the right (west) side impacted only 0.7 ms later. After both sides had contacted the surface, the test article experienced downward deformation, which was like the behavior seen in the flatwise test. The downward deformation can also be shown in the upward facing surface, with noticeable downward, concave deformation at approximately 1.8 ms after impact. The test article rebounded shortly thereafter and was airborne due to the rebound at approximately 4.9 ms after impact. It came to rest, on its side shortly thereafter. The test article in its post-test position is shown in Figure 10.

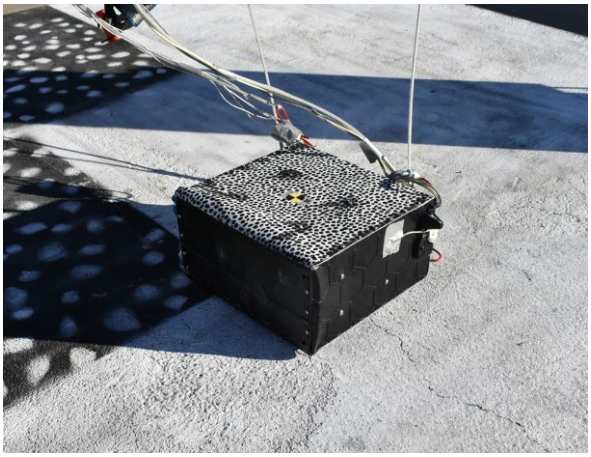

Figure 10 - Post-test position, Rightside Up orientation

The filtered acceleration plot is shown in Figure 11.

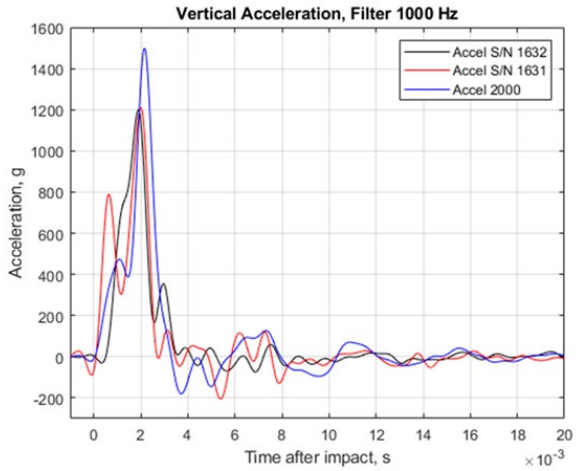

Figure 11 - Acceleration from right-side-up orientation

Unlike the previous test, the acceleration shapes and timing between all three accelerometers were similar and confirmed an approximate 3 to 3.5 ms pulse duration, which also confirmed a nominal impact condition was present. The peak accelerations occurred between 1.8 ms for SN 1631 and 2.1 ms for SN 1632 after impact. Accelerometer SN 1631 did record localized peak acceleration of approximately 788 g prior to the 1.8 ms time, indicating that it was on the side of the test article that made the initial contact with the impact surface. When examining the peak values, while slightly different in peak magnitudes, generally agreed between corner and middle accelerometers, noting the corner accelerometers measured the approximate same acceleration peak values. The accelerometers mounted in the corners measured 1,210 g and 1,199 g for accelerometer SN 1631 and SN 1632, respectively, while Accel 2000 measured a peak value of 1,498 g, which was slightly higher than the corners, but similar. There were no noticeable events that occurred after the initial impact, and thus the loading of the test article all occurred in the 3 to 3.5 ms window.

The post-test diagnostics were able to confirm readings for post-test voltages and temperatures indicating connectivity was present in the module post-test. This result suggested the internal damage (if any) in the module was minor enough to allow for the internal connections to be intact, or in areas that would not affect the connectivity for the diagnostics. The thermocouple data did not show any significant temperature rise in the test articles post-test, so it was determined no TR was occurring. However, per the test procedure, the module was left in outside storage for monitoring for a period of 24 hours. After the 24-hour monitoring period, the test article was ready for post-test forensics.

Upside Down Orientation

The test article in the Upside Down orientation featured the vent facing downward toward the impact surface and oriented such that the positive electrode was facing East. The stochastic pattern was applied to the positive electrode and cooling plate sides. Accelerometer SN 1631 was placed on the northwest corner while accelerometer SN 1632 was placed on the southwest corner. This was the only test conducted where the accelerometers were not placed on opposite sides and was set up this way due to constraints in the attachment cabling. Accel 2000 was placed in the middle of the bottom surface of the enclosure, near the west edge, which was an upward facing surface for this orientation. The test was conducted on November 13, 2023, at 4:41 PM local time. The outside temperature was 69.6° F with a relative humidity of 40.7 %. Winds were 4.3 MPH. The test article impacted at the north-west corner, with a north-side low angle of 6.2 degrees, west-side low angle of 2.3 degrees and an impact velocity of 48.5 feet per second (ft/s). The test sequence is presented in Figure 12.

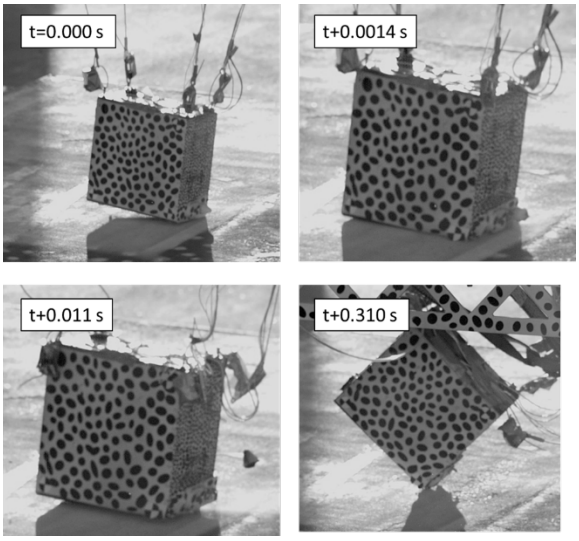

Figure 12 - Test sequence – Upside Down orientation

The north side made initial contact with the impact surface first and began to crush. The test article crushed enough so that the south side made contact

approximately 1.4 ms later. Unlike the flatwise test, there was no rotation of the test article due to the slightly off-nominal impact, so it retained its pre-impact orientation. After the southside contact, the test article rebound began approximately 11 ms after initial impact, after which it became restrained by the attachment cables which caused it to rotate slightly, and then recontact the impact surface 0.31 s on the north corner. It came to rest in its original Upside Down orientation a short time later. The test article in its post-test position is shown in Figure 13.

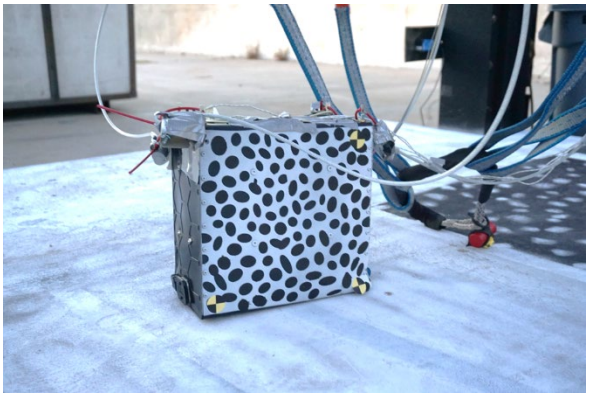

Figure 13 - Post-test position, Upside Down orientation

The filtered acceleration plot is next shown in Figure 14.

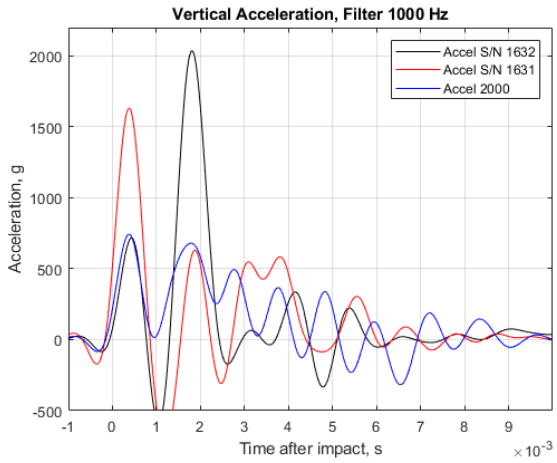

Figure 14 - Acceleration from Upside Down orientation

The acceleration results show two distinct events occurring – one at impact and one approximately 2 ms after impact. The event occurring at impact is in accelerometer SN 1631 which was located on the northwest corner and confirmed the north side of the test article made the initial impact with the surface. Accelerometer SN 1632 data exhibited a spike at approximately 2 ms after impact, which also confirmed the approximate timing of the south side contact. These two peaks were also recorded by accelerometer 2000, though the magnitudes were much smaller due to its location being away from the impact surface However, there appeared to be some additional response in the acceleration results noting there was non-zero acceleration that appeared to be sustained up until approximately 10 ms after initial impact. Examination of the high-speed camera data confirms that there was a crush response in the test article that lasted approximately 11 ms during the impact, so the results measured by the accelerometers aligned with the crushing of the test article. Since Accel 2000 was less affected by the localized spikes, it was analyzed further to obtain the global response of the test article during the crush. This data is presented next in Figure 15.

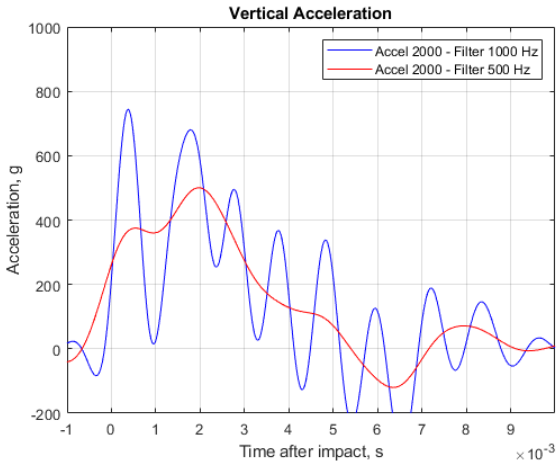

Figure 15 - Vertical acceleration from Accel 2000 using two cutoff frequencies

Accelerometer 2000 was plotted first at the previously determined filtering scheme with 1000-Hz cutoff frequency. There appeared to be an underlying pulse shape present, so the data was refiltered and replotted at the lower 500-Hz cutoff frequency, which is shown as the red curve in Figure 15. Using the 500 Hz filter, the accelerometer measured a triangular pulse shape with peak magnitude of 500.2 g, with a duration of approximately 6 ms. This is slightly shorter than the 11 ms crush duration noted from the video however determining precise timings for the image sequence was difficult due to the short duration of the events and the limited frame rate of the cameras. In either case, the general trend remained.

The post-test diagnostics were not able to confirm post-test voltages and temperatures suggesting that connectivity was lost during the test due to internal damage. However, a multimeter was used to collect manual measurements, and these showed a short between the positive electrode to the module chassis confirming internal damage and/or deformation had occurred. However, the manual measurements also showed a positive to negative terminal voltage of 32.9 V indicating at minimum there was still connectivity between the cells. The thermocouple data did not show any significant temperature rise in the test articles posttest. After the test, per the procedure, the module was placed in outside storage for the 24-hour observation period. After the 24-hour monitoring period, the test article was ready for post-test forensics. Test articles from the flatwise, Rightside Up, and Upside Down tests are shown in the outside storage container, in Figure 16.

Figure 16 - Test articles in outside storage

Sideways Orientation

The Sideways orientation positioned the side with the positive electrode facing the impact surface and oriented it with the vent tube facing North. Accelerometer SN 1631 was placed in the northeast corner of the test article while SN 1632 was placed in the southwest corner. Accel 2000 was placed in the middle of the upward facing surface. The bottom and flat side opposite the cooling plate were painted with the stochastic pattern and the test article was attached to the trolley via cables attaching to the upward facing side. The Sideways orientation test was conducted on March 13, 2024, at 9:07 am local time. It was not conducted at the same time as the others due to availability of the module. However, the test setup which included the lifting configuration, instrumentation and test conduct were identical to the others. The outside temperature was 53.9° F, the wind was calm and relative humidity was 61.5%. The test article impacted nominally along the west edge, with a west-side low angle of 6.5 degrees and an impact velocity of 50.6 feet per second (ft/s). The test sequence is shown in Figure 17.

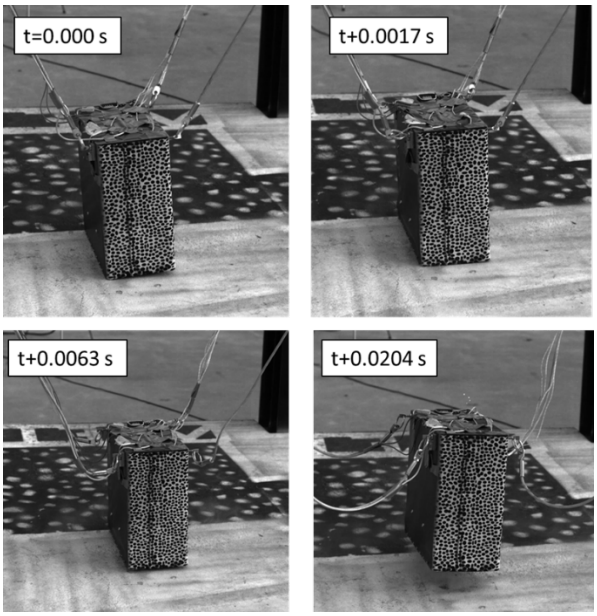

Figure 17 - Test sequence – Sideways orientation

The bottom of the test article is facing the camera view and the darker vertical line approximately midway down the test article is a seam in the outer enclosure. The test article impacted the concrete at a slight west-low orientation, however with the positive electrode protruding from the northeast corner of the test article (facing the impact surface), both the west side and the electrode impacted at approximately the same time. For the next 1.7 ms after the initial impact, the top facing side of the test article experienced an inward deflecting motion until maximum deflection was reached. After maximum deflection, the rebound began with the top facing side returning to an approximate level orientation with only slightly outward bowed deformation. While the rebound occurred, sparks appeared out of the negative electrode, suggesting that an internal short occurred at or just prior to this time. The sparks began to occur approximately 6.3 ms after the impact and continued to be seen until 8.2 ms after impact. Finally, the bottom right image shows the test article in the midst of its post-impact rebound. The test article recontacted the impact surface approximately 0.639 s after initial impact and eventually came to rest in its original test orientation post-test. The post-test position of the test article is shown in Figure 18.

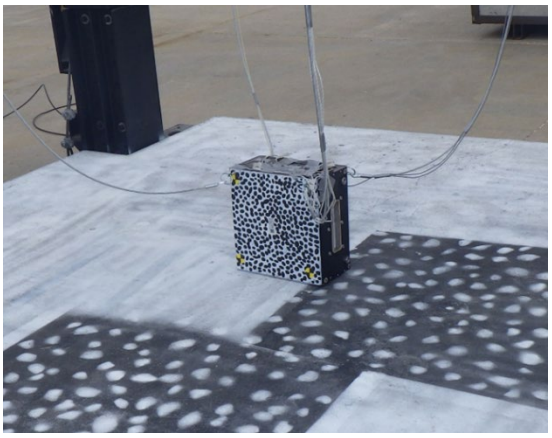

Figure 18. Post-test position, Sideways orientation

The filtered acceleration plot is next shown in Figure 19.

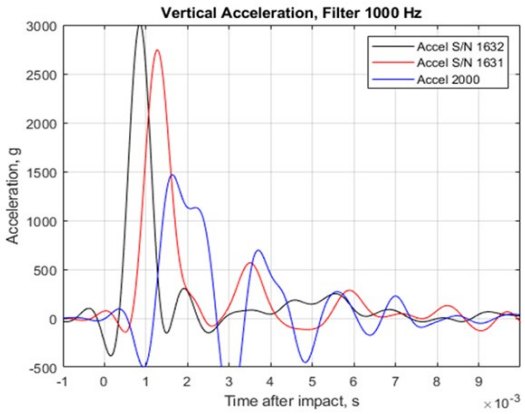

Figure 19 - Acceleration from Sideways orientation

The acceleration data shows two large spikes in the accelerometers mounted in the corners of the test article. The magnitudes are approximately 3013 g for accelerometer SN 1632 which was located on the southwest corner of the test article which saw initial impact, and 2744 g for accelerometer SN 1631 which was located on the northeast corner. The magnitudes are spaced approximately 0.42 ms apart. The duration for southwest corner accelerometer was approximately 1 ms, while the duration of the northeast accelerometer was between 1.3 and 1.5 ms. The timing generally followed the impact sequence shown in Figure 17, however determining precise timings for the image sequence was difficult due to the short duration of the events and the limited frame rate of the cameras. Accel 2000 recorded approximately a 1465 g peak value, which occurred 0.37 ms afterward. The two accelerometers mounted in the corners of the test article did not see any other significant events from the test, while the accelerometer located in the middle of the test article experienced a post-impact oscillation type response with decay. This oscillation was due to the dynamics in the outer surface in which it was mounted.

Connectivity measurements were not able to be recorded post-test using the diagnostic monitor connected into the communication port, suggesting damage or deformation to the internal components. Terminal to terminal voltage was not measured. The thermocouple data did not show any significant temperature rise in the test articles posttest. Per the procedure the test article was placed in outside storage for observation for a period of 24 hours. After the 24-hour monitoring period, the test article was ready for post-test forensics.

After the tests were completed, the collected accelerations were plotted for all of the tests to allow for comparisons to occur. The first set of data is for an accelerometer located at the corner of the test article which impacted first for each of the tests conducted. These data are shown in Figure 20.

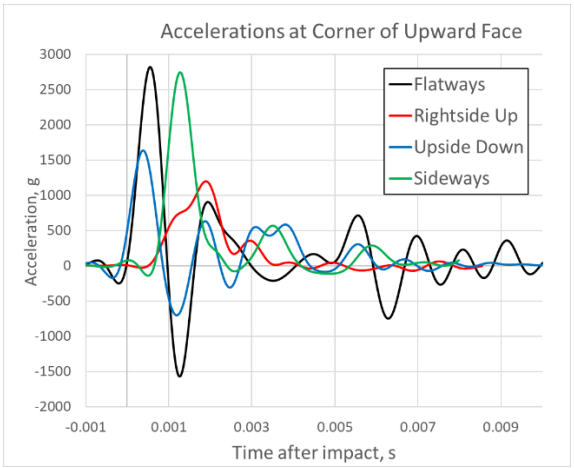

Figure 20 - All test acceleration, corner location

The corners of the modules provide a range of responses in both magnitude and duration of the measured accelerations. This range is due to characteristics regarding the local stiffness in a module's particular orientation (i.e. the orientation of the pouch cells requires more support structure) along with to a lesser extent, the conditions tested (i.e. impact orientation and velocity). To elaborate on the local stiffness, the accelerometers on the Flatwise and Sideways tests were mounted on corners of the side

faces of the modules. The "side" nomenclature represented the faces as either containing the placard or opposite of containing the placard. In contrast, the tests for the Rightside Up or Upside Down orientations, the accelerometers were mounted on the ends faces of the module. The "ends" nomenclature represented the face containing the vent and the opposite of the face containing the vent. Thus, the two higher range accelerations were measured at similar faces for the tests, while the tests with the two lower accelerations were measured on two different faces for the test, even with the locations being adjacent to each other. These results mean acceleration magnitudes from the end tests must be discussed with these considerations in mind. The accelerations collected from the accelerometer mounted in the middle of the module for all four tests were next examined to provide some comparative results. These data are shown in Figure 21.

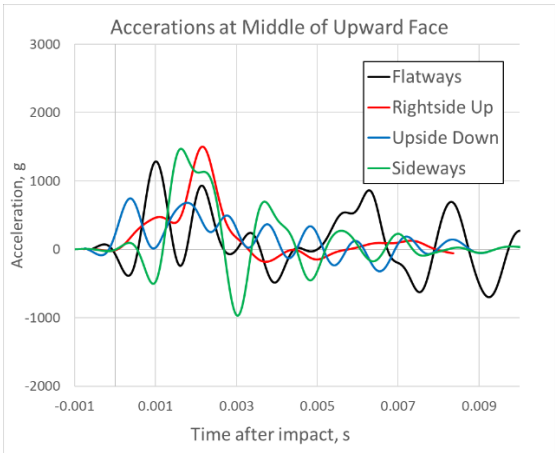

Figure 21 - All test acceleration, middle location

Unlike the accelerations measured at the corners of the modules, the accelerations measured in the middle of the modules matched more closely between the different orientations tested. The differences between the measured response from the middle and the measured response on the corners is based on a variety of factors. The first is that for some tests which impacted with significant off-nominal angle, the corner accelerometer would measure a high value due to the point loading condition from the impact. Secondly, their location at the corners positioned the accelerometers at the most rigid locations on the test articles, due to the end and side faces being joined at these locations. For the middle accelerometers, in three of the four tests, they were placed on the upward facing surface, typically in the middle near the standoff fasteners which attached the outer enclosure to the inner cell containment enclosure assembly. Since there was no method to instrument the cell containment assembly, measurements from the middle accelerometer were generally taken as the best available indicator of what was occurring in the module's cells as it was nearest to the cell attachment locations. In the Rightside Up test, because the vent was present, the middle accelerometer was mounted on the side of the upward facing top surface, and thus provided a similar result to the corners. Examining the numbers, the Upside Down orientation produced the lowest peak accelerations measuring a value of 743 g, while the other orientations generally were in agreement at 1,286 g, 1,498 g, and 1,467 g for Flatwise, Rightside Up, and Sideways, respectively. While there is some room for interpretation, the Upside Down orientation general pulse shape appeared to be trapezoidal to square in nature, which contrasted the other three orientations. For the other three orientations, the general shapes were triangular in nature. The longer, more defined and lower magnitude pulse shape from the Upside Down case likely represented the sustained acceleration during the outer enclosure crushing, while the other three orientations experienced much less sustained motion, which resulted from much less crushing in the enclosure. The deformation results will be examined in detail in Part 2 to provide additional insight into this behavior. All in all, the environment was still a shock-type environment, falling generally out of family with acceleration magnitudes and durations typically seen in responses from crash testing [12].

SUMMARY

Four tests were conducted on four energy storage modules in various orientations in order to examine failure modes that occur, effect of the orientation of the test article, and performance under a 50-ft vertical impact test. The modules were in a zero state of charge configuration, and without external attenuation or structure.

The accelerations generated from the tests show extremely high magnitude, low duration, shock-like pulse which fall out of family with typical crash data. Peak accelerations ranged between 743 g to almost 1,500 g in locations in the middle of the module. None of the modules tested entered TR and post-test diagnostics on the Rightside Up and Flatwise test articles revealed that the mechanisms providing the diagnostic information were still intact and functioning, suggesting the internal damage (if any) did not interfere with the functionality of these

systems. Diagnostics were unable to be completed on the modules that were oriented Upside Down and Sideways for the tests.

After the tests were conducted, each module was disassembled and detailed examinations on each of the internal components were conducted. Items such as cell puncture or breach, electrolyte leaks, or shorting of the internal components were all noted in some of modules, and it is items such as these that can all contribute to the enhanced probability of TR. So, while definitive statements regarding the change of TR cannot be made, the results of the examinations were graded using a common scoring rubric in an attempt to quantify damage. These results will be presented in Part 2.

DISCUSSION

The tests conducted on the modules were intended to generate data to aid in discussions regarding ESS under dynamic loads resulting from a 50-ft drop test to support ESS certification efforts. The tests resulted in differing responses in the modules, which was largely dependent on the orientation tested. There were failures in the modules (described in Part 2) that were results of specific test conditions, which were recorded to provide discussion into the correlation (or lack thereof) between loading environment and damage type and level.

While test efforts were deemed successful in proving data that can be used in discussion, it should be noted that the tests were conducted on a specific make of ESS containing a single type of cell architecture (pouch cells) and it is understood that other architectures and design factors may perform differently. On the other hand, there are many common factors amongst the various architectures developed, so application of some of the results for various types of systems and installations could be considered, albeit using proper context.

The overall research objectives within the RVLT Project intend to conduct the study in three phases, with each subsequent phase building on the knowledge gained from previous tests. This report describes this first phase of tests. In this phase, ESS modules were configured without structure, without connections, and without supporting systems such as the Battery Management System (BMS) in order to isolate the response of the module itself to test for considerations previously discussed in this report.

The second phase, which was conducted in 2024, tested the modules with attenuation in two of the orientations presented here, as a way to replicate, to a certain extent, an installed configuration, while still being vehicle agnostic. The third phase intends to build off of the knowledge gained and test energized modules and is still in formulation.

AUTHOR CONTACT

Justin Littell, Justin.D.Littell@nasa.gov

Nathaniel Gardner, Nathaniel.W.Gardner@nasa.gov

Shay Ellafrits, Shay.A.Ellafrits@nasa.gov

ACKNOWLEDGEMENTS

The authors would like to thank Rob Huculak and his test team at NIAR for conducting the 4 drop tests. In addition, the authors would like to thank Joseph James, Spencer Wright, Derek Larsen and at Brad Mowry at EPS for the support and guidance on the ESS module technical data and for assisting in post-test forensics.

.

REFERENCES

1. Code of Federal Regulations. “Fuel System Crash Resistance.” 14 CFR §27.952. October 3, 1994.

2. Federal Register. “Airworthiness Criteria: Special Class Airworthiness Criteria for the Joby Aero, Inc. Model JAS4–1 Powered-Lift.” Volume 87, No. 215. Pages 63799-67413. November 8, 2022.

3. Federal Register. “Airworthiness Criteria: Special Class Airworthiness Criteria for the Archer Aviation Inc. Model M001 Powered-Lift.” Volume 87. No. 243. Pages 7749-77763. December 20, 2022.

4. Federal Aviation Administration. “Designation of Applicable Regulations.” 14 CFR §21.17. Amended February 16, 2024.

5. EASA. “Means of compliance with the Special Condition VTOL.” MOC-SC-VTOL Issue: 2. May 12, 2021.

6. Littell, J.D., Gardner, N.W. and Ellafrits, S.A. “Dynamic Drop Testing of eVTOL Energy Storage Systems Part 2: Deformation and Post-Test

Forensics Results." Proceedings from the Vertical Flight Society 81st Annual Forum. Virginia Beach VA. May 20-22, 2025.

7. Federal Aviation Administration. "Technical Standard Order: Rechargeable Lithium Batteries and Battery Systems." TSR-C179b. March 23, 2018.

8. United Nations. "Manual of Tests and Criteria, Seventh Revised Edition." ST/SG/AC.10/11/Rev 7. 2019.

9. Littell, J.D., Gardner, N.W., and Ellafrits, S.A. "Dynamic Testing of eVTOL Energy Storage Systems: Literature Review and Path Forward." NASA TM 20220015117. January 2023.

10. NIAR-WSU. "NIAR conducts 50-ft eVTOL battery drop test per 14 CFR § 27.952." December 2, 2022. https://www.wichita.edu/industry_and_defense/NIAR/MediaCenter/2022-12-22.php. Accessed March 28, 2024.

11. Society of Automotive Engineers (SAE). "Surface Vehicle Recommended Practice: Instrumentation for Impact Test-Part 1-Electronic Instrumentation." SAE J211-1. 2007.

12. Littell, J.D. and Putnam, J.B. "A Summary of Test Results from a NASA Lift + Cruise eVTOL Crash Test." Proceedings from the Vertical Flight Society's 70th Annual Forum. West Palm Bean, FL. May 16-18, 2023.